Oxidation states and ionicity

Aron Walsh[1,2], Alexey A. Sokol[3], John Buckeridge[3], David O. Scanlon[3,4], and
C. Richard A. Catlow[3,5]

[1]Department of Materials, Imperial College London, London SW7 2AZ, UK
[2]Department of Materials Science and Engineering, Yonsei University, Seoul 03722, Korea
[3]Department of Chemistry and Thomas Young Centre, University College London, London WC1H 0AJ, UK
[4]Diamond Light Source Ltd., Harwell Science and Innovation Campus, Oxfordshire OX11 0DE, UK
[5]School of Chemistry, Cardiff University, Cardiff CF10 3AT, UK

The concepts of oxidation state and atomic charge are entangled in modern materials science. We distinguish between these quantities and consider their fundamental limitations and utility for understanding material properties. We discuss the nature of bonding between atoms and the techniques that have been developed for partitioning electron density. Whilst formal oxidation states help us count electrons (in ions, bonds, lone pairs, etc.), variously defined atomic charges are usefully employed in the description of physical processes including dielectric response and electronic spectroscopies. Such partial charges are introduced as quantitative measures in simple mechanistic models of a more complex reality, and therefore may not be comparable or transferable. In contrast, oxidation states are defined to be universal, with deviations constituting exciting challenges as evidenced in mixed-valence compounds, electrides, and highly-correlated systems. This Perspective covers how these concepts have evolved in recent years, our current understanding, and their significance.

The concept of *oxydationsstufe* was developed over two centuries ago to describe the observed reactions of elements with oxygen[1]. Such chemical reactions are quantised, with distinct changes in structure and properties as more oxygen is bound by an element (e.g. $6\mathrm{Fe} + 3\mathrm{O}_2 \to 6\mathrm{FeO} + \mathrm{O}_2 \to 2\mathrm{Fe}_3\mathrm{O}_4 + \frac{1}{2}\mathrm{O}_2 \to 3\mathrm{Fe}_2\mathrm{O}_3$). The modern oxidation state is defined as "the degree of oxidation of an atom in terms of counting electrons", where the nominal counting of electrons is performed following an agreed-upon set of rules[2].

This Perspective focusses on chemical bonding in solids, where discussion almost invariably makes reference to oxidation states, ionicities, covalency, and charge distributions, which are indeed powerful concepts across the chemical sciences. Despite their widespread use, however, there are uncertainties and ambiguities about the concepts and their interrelationships. The debate became so heated in the 1960s that there was a sequence of three publications in Nature on this topic arguing different perspectives: Goodman discussed the role of atomic electronegativity in the distribution of electrons in solids[3]; Mooser and Pearson emphasised that bond ionicity is a theoretical concept that depends on the approximation employed[4]; while Cochran focused on what can and cannot be measured in practice[5].

As argued previously, the concept of ionicity in solids remains intrinsically ambiguous[6]: charge distributions can be calculated and measured with growing accuracy, but there are several different plausible schemes for their partition between the component atoms. Alternative definitions and measures of ionicity are necessary to describe other properties, for example dielectric response, which depend on charge distribution. Further difficulties arise when the equilibrium charge distribution is linked to oxidation state. We may agree

47 that a molecule or solid has a metal in its highest accessible oxidation state, but experiment
48 and theory will often reveal significant electron density in its valence shell orbitals.

49 Debate continues on the topic and is indeed very much alive[7–10]. We attempt to address
50 these problems and to show how ionicity, charge distribution, and oxidation state
51 interrelate and can be meaningfully used. We further discuss cases where genuine
52 ambiguities and challenges exist for mixed-valence compounds, as well as new generations
53 of quantum materials at the frontier of materials science.

54 Utility of Formal Oxidation States

55 Electron counting is at the heart of our understanding of, and approach to, chemical
56 bonding[11]. In one trivial example, two hydrogen atoms (one-electron species) interact
57 through a two-electron covalent bond formed by filled bonding and empty anti-bonding
58 orbitals. In the solid state, a similar case would be crystalline silicon, where two-electron
59 two-centre covalent bonds are formed between nearest-neighbour silicon atoms in a
60 periodic structure. In both cases, effective charges are usually assumed to be zero. The
61 valence number can however be defined as I (hydrogen) and IV (silicon), which represents
62 the number of electrons involved in (or available for) chemical bonding.

63 The combination of a metal with a more electronegative element can be described by the
64 formation of an ionic (or heteropolar) bond. One such case is LiF, where one-electron
65 transfer from Li ($1s^2 2s^1$) to F ($2s^2 2p^5$) results in closed-shell Li^+ ($1s^2 2s^0$) and F^- ($2s^2 2p^6$)
66 electronic configurations. While one can assign different effective charges to Li and F, the
67 formation of a complete closed shell around F and the depletion of the valence charge
68 density around Li are unambiguously detected by experiment and electronic structure
69 calculations. Perhaps, the most important observation here is that the electron associated
70 with Li and all of the originally five p electrons of F take part in the resulting valence shell of
71 the compound. Following simple octet rules for forming a closed-shell (diamagnetic)
72 compound, the outcome we described can trivially be predicted for more complex chemical
73 compounds.

74 These examples of both covalent and ionic interactions can be conveniently described using
75 formal oxidation states. The value of oxidation state for each atom in a solid can be assigned
76 following a set of rules (see Box 1), e.g. the oxidation state of an atom in its elemental
77 standard state is 0. A less trivial example is a multi-component solid such as the high-
78 temperature superconductor $YBa_2Cu_3O_7$. Here, the oxidation state of O is -2, which means
79 that the sum of oxidation states for Y + 2Ba + 3Cu = 14 to provide the electrons involved in
80 the bonding with oxygen. The common oxidation state of Y is +3, that of Ba is +2, so seven
81 electrons need to be donated by three Cu atoms (assuming complete reduction of oxygen).
82 The common oxidation states of Cu are +2 as in cupric oxide (CuO) and +1 in cuprous oxide
83 (Cu_2O). The unusual electron count in $YBa_2Cu_3O_7$ requires either an additional electron
84 (oxidation) from Cu to the +3 state or a hole stabilised on oxygen – often described as a
85 polaron – which leads to its exotic condensed matter physics[12]. This conclusion is made in
86 the absence of any substantial input from theory or experiment, but is crucial in
87 understanding the properties of the material, and demonstrates the importance and power
88 of these simple approaches.

89 While these concepts are easily transferable to the important area of mixed-anion
90 compounds[13], more involved consideration of the structure and bonding is required for the
91 cases of polyion systems, where groups of atoms form sub-units that carry a formal charge.
92 In BaSi, the usual oxidation states of Ba +2 and Si -4 fail to deliver a charge neutral

93   stoichiometric unit; however, the structure contains chains of covalent Si-Si bonds, where
94   each Si adopts a -2 oxidation state. For Ba_3Si_4, discrete Si_4^{6-} polyanions are formed with
95   internal Si-Si bonds, which ensures charge neutrality when combined with thee Ba +2
96   cations. There have been recent applications of such Zintl compounds in the field of
97   thermoelectrics[14,15].

98   Beyond predicting the outcomes of chemical reactions and the stoichiometry of compounds,
99   oxidation states also have a utility in the description of physical properties. Oxidation states
100 underpin a number of successful heuristic tools in molecular and solid-state chemistry,
101 including the valence-shell electron-pair repulsion (VSEPR) theory for predicting structure[16],
102 and ligand and crystal field theory for predicting structure and spectroscopic response, in
103 particular of transitional metal complexes and materials[17]. One example is Mn, of which
104 there are seven positive oxidation states, where Mn(VII) corresponds to the removal of all of
105 the valence electrons and formal configuration of $3d^0$. In the solid state, MnO corresponds
106 Mn(II) ($3d^5$), where the high spin state of $5/2\hbar$ is observed, while MnO_2 contains Mn(IV)
107 ($3d^3$), with a corresponding high spin state of $3/2\hbar$. The intermediate case of Mn_2O_3 contains
108 Mn(III) ($3d^4$), which is Jahn-Teller active and results in a frustrated magnetic interactions in
109 its ground state bixbyite crystal structure[18]. Each of these oxidation states of Mn can be
110 easily distinguished from their distinct spectroscopic and magnetic signatures[19].

111 Assigning formal oxidation states allows us to understand and rationalise key properties of
112 the materials, but it is not a statement about effective charge: assigning an oxidation state
113 of +7 to Mn in, for example, the compound $KMnO_4$ does not imply, as argued above, that a
114 calculated or experimentally measured charge density analysis will find zero charge density
115 in the 3d orbitals; but it does indicate that all the 3d electrons are directly involved in
116 bonding (interaction) with oxygen. Similarly Ti is in oxidation state +4 in TiO_2 as explored in
117 Figure 1; although, there is again appreciable electron density in the Ti 3d orbitals due to
118 bond polarisation and weak orbital hybridisation as observed in the electronic density of
119 states. The next section will explore these ideas in greater depth.

120 Determining and Understanding Partial Charges

121 The historical description of chemical interactions, or bonding, involving the sharing and
122 transfer of integral numbers of electrons was challenged following the development of
123 quantum mechanics. The distribution of electrons in chemical systems is described by the
124 many-electron Dirac equation; however, practical treatments require simplification[20].
125 Techniques employing one-electron wavefunctions are ubiquitous in quantum chemistry,
126 and for solids these take the form of periodic (Bloch) functions. By their nature, these
127 functions are delocalised in real space and cannot be easily interpreted in terms of
128 individual chemical interactions (covalent bonds, lone pairs, etc.).

129 The link to chemical intuition can be recovered by employing one-electron *localised* orbitals
130 (e.g. obtained with Foster-Boys and Pipek-Mezey schemes in molecules and Wannier
131 orbitals in solids, as discussed further below)[21]. However, the complexity of chemical
132 bonding in many compounds necessities going beyond a one-electron picture, *e.g.* in the
133 chemistry of radicals with multi-centre multi-electron interactions. More generally,
134 electrons can be separated into groups, with strong correlation within a single group, and
135 weak correlation between them[22,23].

136 Both experiment and electronic structure based computational techniques are widely used
137 to obtain electron density maps in solids, with a variety of procedures used to interpret
138 them in terms of atomic charges. However, individual atomic charges in a multi-electron

139 compound are not a quantum mechanical observable and there is a high degree of
140 ambiguity both in their definition and in the approaches to calculating them[6], in contrast to
141 the simpler and heuristic oxidation state. Nevertheless the concept of partial (atomic)
142 charges is a useful one and we consider briefly the ways in which it has been formulated and
143 applied.

144 Determining the electronic density associated with a particular atom or ion in a solid-state
145 material is in some ways a natural choice to calculate the atomic charges. Indeed,
146 experimental techniques such as X-ray diffraction (XRD) allow one to measure such
147 densities, and visualise them in real space via a Fourier transform. Information obtained
148 from local surface probes including scanning tunnelling microscopy (STM) and atomic force
149 microscopy (AFM), while limited, can also be used to reconstruct charge density
150 distributions. At the same time, theoretical techniques provide increasingly accurate
151 electron density maps in solids. The crucial question then remains: how are these electronic
152 densities, which are continuous functions through the unit cell of a crystal, partitioned
153 amongst the constituent atoms? In the vast majority of cases, there is overlap in density
154 between atoms, making the partitioning a non-trivial problem.

155 A simple approach is to use geometric partitioning, where the charge within a certain radius
156 or polyhedron, or, in the analysis of Bader[24], within a contour of zero density gradient is
157 computed and associated with an atom. An alternative approach is to construct a set of
158 Wannier functions to associate electrons with each atom[25]; these are Fourier transforms of
159 Bloch wavefunctions onto discrete centres[26]. These sets of Wannier functions are then
160 assigned to ionic cores via their spatial proximity. Unfortunately, such methods only provide
161 a unique and unambiguous definition of atomic charge when both the orbital overlap and
162 polarisation due to electrostatic fields is zero. Partial charges of real materials vary with the
163 method employed and the values are difficult to rationalise in terms of integral electron
164 transfer. A range of such approaches are illustrated in Figure 2 for the case of CdO.

165 The overlap in electron density between atoms can be accounted for through analysis of the
166 electronic wavefunctions in terms of localised, atom-centred basis functions. Through a
167 linear combination of atomic orbitals (LCAO) approach, Mulliken's analysis[27] represented
168 the atomic charge in terms of populations of atomic orbitals. Each pair of atoms has a gross,
169 net and overlap population, given in terms of the atomic orbital basis set. Originally the
170 overlap population was divided equally between the interacting ions, but subsequent
171 improvements on this method have been applied including those of Christoffersen[28]
172 employing molecular orbitals and Hirshfeld[29] using the charge density, which take into
173 account to some degree the polarity of the bond between the atoms. Wavefunction-derived
174 properties, such as the single and pair electron densities have been incorporated in the
175 electron localisation function (ELF, see Figure 2c)[30], which describes the probability of
176 finding an electron close to another in the same spin state and allows one to determine
177 regions where electrons are localised close to atomic centres[31]. Electronic wavefunction
178 analysis, however useful, cannot solve the fundamental problem that atomic charge in
179 compounds is not an observable. Results from such analyses vary strongly with the choice of
180 basis function and with the method used to determine interactions between atoms,
181 whether through LCAO parameterised tight-binding methods or *ab initio* techniques.

182 A crucial consideration when modelling atomic charge is the polarisability of the ion in
183 question. When an electric field is applied to a material, the ions respond not just by
184 changing their centre of mass coordinates, but also by deformation of their electron clouds.
185 Displacement upon ionic polarisation can be accounted for in a simple manner, to describe

186 the response to applied electric fields, by attributing an effective charge to the ion. Good
187 agreement with experimental measurements that probe the dielectric response of a
188 material can be achieved with this approach[5]. Care must be taken with such effective
189 charges including the frequently-used Born charge, however, as their derivation, while
190 useful when modelling the dielectric response of a material, can often mask the underlying
191 physics. For example, such charges can be used in a rigid-ion model of a crystal to calculate
192 the vibrational (phonon) modes, but in doing so one is explicitly assuming that the ions are
193 non-deformable, which greatly limits the transferability of these models. Moreover, the
194 cohesive energy of a crystal is much less dependent on the polarisability of the constituent
195 ions than are the lattice vibrational properties. The ionic charge that reproduces cohesive
196 energies will generally be different from the effective charge that reproduces vibrational
197 frequencies accurately. This problem can be overcome by using polarisable ions in materials
198 modelling, e.g. described with the shell model[32].

199 Taking into account the electronic polarisability of an ion in a solid can remove some of the
200 ambiguities with regard to defining atomic charges. Indeed, this outcome is expected, given
201 that the link between polarisability and experimentally observable quantities is far clearer
202 than that between the poorly defined atomic charges and experiment. In a dielectric crystal,
203 the dipole moment within a unit cell cannot be uniquely defined owing to the arbitrary
204 choice in the definition of the unit cell as a result of translation symmetry. However,
205 differences in polarisation between displaced (atomic and electronic) configurations, which
206 are the source of experimentally observable quantities, do not depend on the unit-cell
207 choice. The computation of such differences in polarisation is the aim of the 'modern theory
208 of polarisation'[27], in which the electron clouds associated with ions are represented by
209 Wannier functions. The polarisation difference is usually calculated through topological
210 analysis of the electron distribution via the Berry phase formalism, from which the number
211 of Wannier centres (i.e. electrons) that move with a particular atomic displacement can be
212 derived[33,34]. Thus a partitioning of electrons is achieved, which is not based on spatial
213 considerations with respect to ion core coordinates, but on the lattice dynamic distribution
214 of the electronic states. Employing this theory, Jiang et al.[35] obtained ionic partial charges
215 from first-principles calculations that recovered formal oxidation states for each species in a
216 diverse set of systems (LiH, water, $BaBiO_3$ and Sr_2FeWO_6). This approach highlights the link
217 between changes in polarisation and oxidation states that is intuitively satisfying;
218 nevertheless, it remains one amongst several approaches.

219 Experimental techniques that measure electron density suffer from the same ambiguity as
220 electronic structure calculations in partitioning to atomic centres. Alternative techniques
221 can be used to probe atomic charges, beyond those based on measuring the dielectric
222 response of a material already mentioned. In electrochemical processes, ionic charges are
223 exchanged in integer numbers through redox reactions. X-ray photoemission spectroscopy
224 (XPS) is widely used to infer oxidation states via the shifts and splittings of core levels that
225 act as spectral fingerprints. Another probe is the absorption edge in X-ray Absorption Near
226 Edge Structure (XANES) measurements, which increases in energy as the oxidation state of
227 the absorption site increases. Neutron spectroscopy, spin resonance techniques, and other
228 spectroscopic or magnetic measurements can be used to probe unpaired spin densities,
229 which can give information on bonding character and from which details on oxidation states
230 can be inferred[19].

231 It is useful at this point to draw together the threads of our argument. The concept of
232 oxidation state is a simple but powerful one. It relates to electron count and indicates the

233 number of electrons from component atoms that are involved in chemical bonding. Charge
234 density is a distinctive entity, which is accessible from experiment and theory, but whose
235 partition into atomic charges is intrinsically ambiguous. Provided this crucial factor is
236 recognised, it is nevertheless a very useful concept and recent approaches to assigning
237 partial charges tend to align them with oxidation states. Our discussion continues with
238 examples of systems and problems that pose particular challenges to the twin concepts of
239 atomic charge and oxidation state.

240 ## Challenges for Mixed-Valence and Correlated Systems

241 The ongoing debate on oxidation states in more complex or complicated systems keeps the
242 field open for further refinement. Oxidation states are straightforward to assign in systems
243 where atoms display a single oxidation state, but they can start to blur in polyion and mixed-
244 valence compounds, where elements are present in more than one distinct state. Imagine a
245 system where metal M exists in oxidation states (A and B), occupying two detectable sites in
246 the crystal (labelled X and Y). The degree of mixing between these two Heitler-London
247 configurations $M_X^A M_Y^B$ and $M_X^B M_Y^A$ will be controlled by how distinguishable the two
248 crystallographic sites are[36]. Robin and Day categorised these systems into three classes[37]: (i)
249 Class 1, where the sites are very different and the electrons are completely trapped, (ii)
250 Class 3, where the sites are indistinguishable and the system has a genuine non-integral
251 oxidation state, and (iii) Class 2, where the sites are distinguishable, however, not very
252 different, and so a range of intermediate oxidation state behaviours can be observed.

253 Class 1 compounds should be the easiest to understand; however, the assignment in some
254 systems still promotes debate. Silver monoxide, (AgO or Ag_2O_2) is one such example, where
255 Ag exists in the +1 and +3 oxidation states, with Ag(I) in a linear coordination between two
256 oxygen, and Ag(III) in a distorted square planar coordination. Despite these different
257 crystallographic sites, assignment of the oxidation states present in AgO has been
258 contentious, with some studies favouring an explanation of Ag(I),Ag(II) with localised hole
259 polarons on oxygen. This controversy was solved using electronic structure calculations in
260 tandem with X-ray photoemission and fine-structure analysis[38]. Another Class 1 system,
261 covelite (CuS) is a mineral in which Cu is found in two distinct coordination environments
262 (trigonal planar and tetrahedral) and S is also found in different environments, with one
263 third of the S in a trigonal pyramidal coordination and two thirds present in S—S dimers.
264 Counter to chemical intuition, the oxidation state of Cu in CuS is thought to be Cu(I) due to
265 the presence of the S_2^{2-} dimers; although, debate remains as to whether there is a mixture of
266 oxidation states on the Cu sites, on the S sites or on both[39].

267 Temperature can conspire to make the analysis of oxidation states in mixed valence systems
268 difficult. At room temperature, magnetite (Fe_3O_4) crystallises in a cubic AB_2O_4 spinel
269 structure, in which Fe(III) ions occupy the tetrahedral A sites, and a 50:50 ratio of Fe(II) and
270 Fe(III) ions occupy the octahedral B sites, which can be difficult to distinguish. Below 125 K,
271 the system undergoes what is known as the Verwey transition, a structural distortion to a
272 monoclinic superstructure, and becomes electrically insulating, with the charge ordering of
273 the similarly-sized +2 and +3 ions contentious for many years. Recently, an investigation by
274 Attfield and co-workers revealed the presence of localised electrons which are distributed
275 over three linear Fe-site units, termed trimerons[40]. This breakthrough was enabled by large
276 40-micrometre grains of the low temperature structure, which allowed the identification of
277 the emergent order.

278 Similarly, pressure can change the nature of charge distributions in a solid, making the
279 analysis of oxidation states quite complex. Boron is a metalloid that exists in several well-
280 known allotropes. In nearly all of these allotropes, the structures are made up of icosahedral
281 B_{12} clusters that feature metallic-like three-centre bonds within each icosohedron, and
282 covalent two- or three- centre bonds between the icosahedra, satisfying the octet rule and
283 yielding insulating electronic structures. Under pressures exceeding 19 GPa and less than 89
284 GPa, boron adopts a novel ionic structure, consisting of an NaCl-type arrangement of
285 icosahedral B_{12} clusters and B_2 pairs[41]. The resultant structure is a "boron boride", perhaps
286 best characterised by the formula $(B_2)^{\delta+}(B_{12})^{\delta-}$.

287 Highly-correlated systems can also present a challenge to our understanding of oxidation
288 states. Plutonium – important as a nuclear fuel – is situated amongst the actinides in the
289 periodic table. In the early actinides (Th to Np), the 5f electrons are delocalised, which
290 allows them to take part in bonding within the lattice, similar to the behaviour of the 5d
291 series. For the heavier actinides (above Am), the 5f electrons are localized, and do not take
292 part in bonding. Plutonium is at the cusp of these two behaviours, resulting in one of the
293 most complex electronic structures for an elemental metal[42]. The ground state has only
294 recently been conclusively revealed to be a quantum mechanical admixture of localised and
295 itinerant electronic configurations, with the charge fluctuating between distinct Pu(IV) ($5f^4$),
296 Pu(III) ($5f^5$) and Pu(II) ($5f^6$) electronic configurations[43].

297 The breakdown of simple concepts of oxidation state has also been emerging as a key
298 ingredient in many observations of unconventional critical phenomena, which do not follow
299 standard spin-fluctuation theories. The quantum criticality of Yb-valence fluctuations have
300 been shown to be the origin of divergent spin behaviours in $YbRh_2Si_2$ and β-$YbAlB_4$, $YbAgCu_4$,
301 and $YbIr_2Zn_{20}$,[44] and similarly the valence fluctuations of Ce in $CeIrIn_5$.[45] In superconductivity,
302 nearly critical valence fluctuations has been reported to mediate Cooper pairing in $CeCu_2Ge_2$
303 and $CeCu_2Si_2$ under high pressure[46].

304 These are examples of challenging cases to the oxidation state concept. Situations where
305 the assignments of oxidation states become ill-defined are usually those associated with
306 intriguing new physics that tests our very understanding of chemical bonding in solids.

Outlook

308 With the ever-increasing arsenal of advanced theoretical methods and experimental
309 techniques available at present, the misunderstandings of (and challenges to) our
310 understanding of oxidation states are slowly decreasing. The related but distinct concepts of
311 oxidation state, atomic charge, and ionicity will remain of key importance in understanding
312 and describing chemical bonding in general, but particularly in solids. While modern
313 sophisticated methods may uncover challenges to what are inherently simple and intuitive
314 investigative tools, the concept of oxidation state, which has survived over two centuries of
315 use in the chemical sciences, will stay at the core of our description of the interaction of
316 atoms in molecules and solids, provided the distinctions between it, the atomic charge and
317 ionicity are fully appreciated.
318
319 As our understanding of the structure and properties of diverse materials continues to
320 improve, we expect a clearer view to emerge of electronic and ionic interactions in highly
321 challenging systems including new classes of high-*T* superconductors[47], boron compounds[48],
322 supported metal and semiconductor nanoclusters[49], layered MXenes[50] and beyond. The key
323 concepts in electron group theory, the theory of polarisation, supercritical behaviour, and

324 the integral view of microscopic and mesoscopic behaviour of solids including charge and
325 spin fluctuations are all essential ingredients to the future application and utility of the
326 oxidation state.
327
328

329

330

331
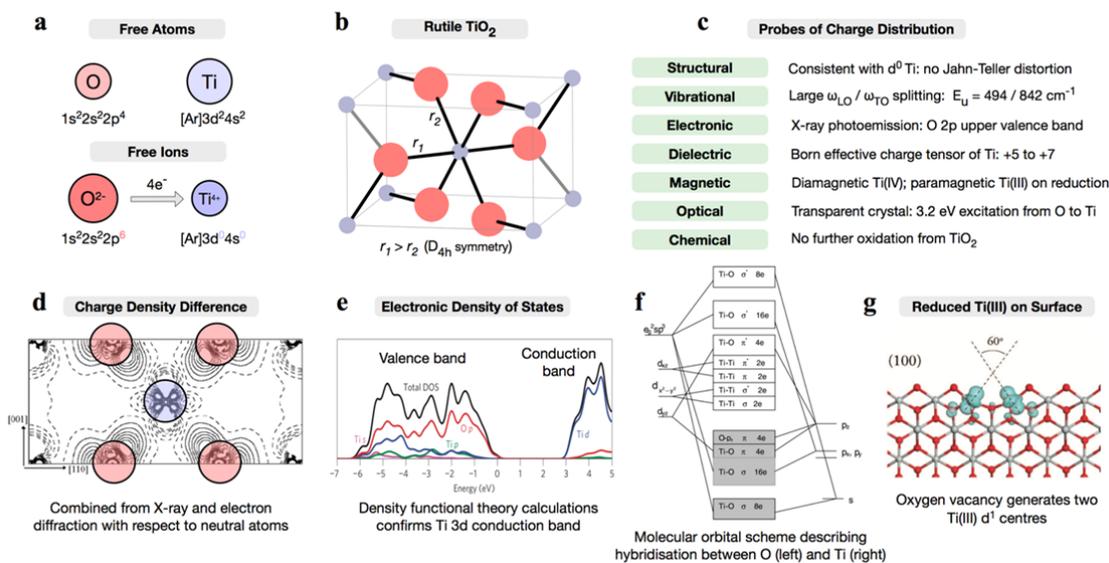
Figure 1 Charge distribution in TiO_2. (a) The formal oxidations states are +4 for Ti and -2 for oxygen. (b) The material adopts a range of polymorphs, but here we focus on rutile, which is one of the most stable. (c) Various experimental probes of the charge density are available; (d) the measured charge density difference confirms a depletion of d orbital density from Ti and a transfer to O [Reproduced from Ref. [51]]. (e) The first-principles electronic density of states demonstrates a conduction band formed of Ti d [Reproduced from Ref. [52]], with hybridisation in the valence band that can be described by (f) a simple molecular orbital scheme[51,53]. (g) Finally, when excess electrons are added to the material or formed via charged point defects, they localise to give paramagnetic Ti(III) d^1 centres as calculated from first-principles and observed in surface measurements [Reproduced from Ref. [54]].

343

344

345
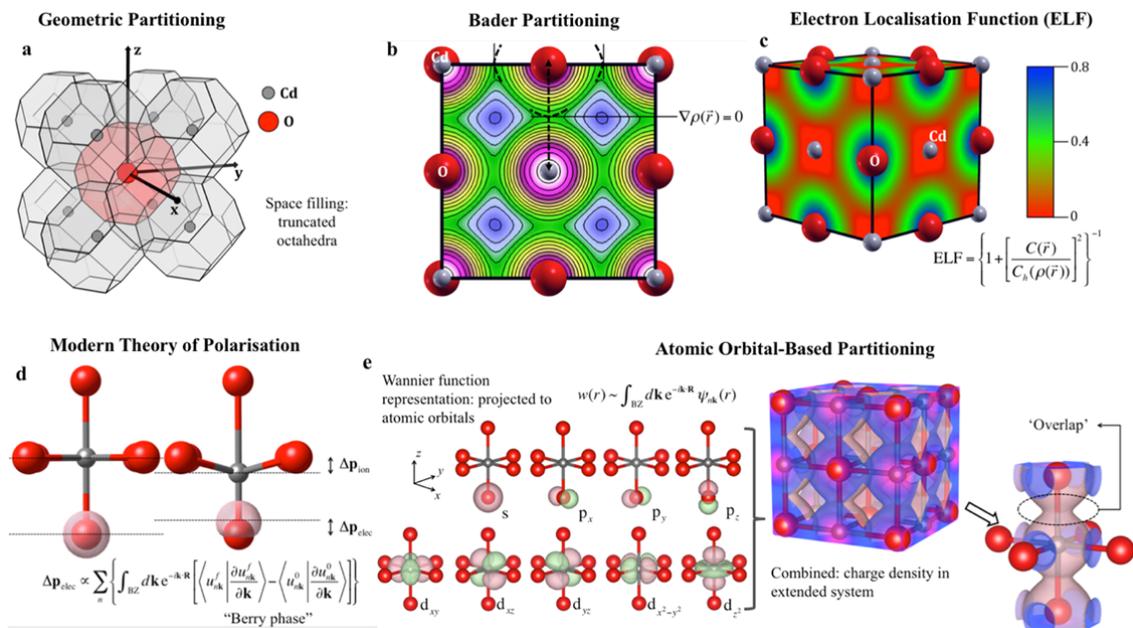
Figure 2 Illustration of five approaches for partitioning electron density between atomic centres in chemical systems. We use the case of CdO, in which Cd has a formal +2 and O has a -2 oxidation state. (a) Geometric partitioning based on space filling for a Wigner-Seitz polyhedral decomposition of CdO in a CsCl-like structure. (b) Topological analysis of the electron density $\rho(\vec{r})$ in rocksalt CdO as shown using Bader's Atoms in Molecules approach. (c) Analysis of electron pair probability distribution as determined using the electron localisation function (ELF – here the functions C and C_h are related to the electron pair density, see Ref. [30]). (d) Changes in electric polarisation $\Delta \mathbf{p}$ from topological analysis of the electron distribution using the Berry phase formalism applied to standard band structure calculations in the Bloch function basis, see Refs. [33,34]. (e) Projection of extended electronic wavefunctions onto localised orbitals (Wannier functions, $w(r)$, defined again using pre-calculated Bloch functions) that combine to reproduce the full electron density of the crystal.

360 **Box 1 Assigning formal oxidation states**

361 The oxidation state represents "the degree of oxidation of an atom in terms of counting
362 electrons" [IUPAC, 2018]. For the simplest cases, the octet (eight electron) rule is sufficient
363 for electron counting, where atoms are assigned octets in order of decreasing
364 electronegativity until all valence electrons are distributed. The resulting atom charge then
365 represents the oxidation state. For example, when Zn ($3d^{10}4s^2$) and O ($2s^22p^4$) are brought
366 into contact to form ZnO, the octet of O is completed ($2s^2p^6$) with oxidation state -2, while
367 Zn adopts a $3d^{10}4s^0$ configuration with oxidation state +2.

368 A set of more general rules for determining oxidation states are provided in undergraduate
369 chemistry textbooks. For example, following those given in "Inorganic Chemistry" [Mark
370 Weller, Tina Overton, Jonathan Rourke, and Fraser Armstrong, OUP, 6th Edition, 2014.]:

371 1. The sum of oxidation states for all atoms in the species is zero to ensure electroneutrality

372 2. Atoms in their elemental form: 0

373 3. The available valence electrons follow the Group in the Periodic Table, e.g.

374   Atoms of Group 1: +1

375   Atoms of Group 2: +2

376   Atoms of Group 3: +3

377   Atoms of Group 13: +1 (filled s^2 lone pair) or +3

378 4. Hydrogen in compounds with nonmetals: +1 (hydron)

379   in compounds with metals: -1 (hydride)

380 5. Fluorine: -1

381 6. Oxygen: -2 unless combined with fluorine

382   -1 in peroxides (O_2^{2-})

383   -1/2 in superoxides (O_2^-)

384   -1/3 in ozonides (O_3^-)

385 7. Halogens: -1 unless other elements include O or more electronegative halogens

386 These rules are sufficient for assigning oxidation states of most solids, but there are caveats
387 and a number of interesting exceptions are discussed in the main text such as in polyion and
388 mixed-valence compounds. Many elements, in particular the transition metals, can exist in a
389 variety of oxidation states.

390 Beyond assignment based on composition alone, as part of crystal structure determination
391 it is common to use knowledge of the local structure (bond lengths and angles) to assign
392 oxidation states based on a valence bond analysis[55]. One assignment algorithm involving
393 analysis of nearest-neighbour coordination environments is implemented in the open-
394 source PYMATGEN package [http://pymatgen.org].

395

396

397

398

Box 2 X-ray Photoelectron Spectroscopic (XPS) fingerprints of oxidation states

The experimental technique of X-ray photoelectron spectroscopy (XPS) is a crucial analytical tool in materials science, which is widely used to assign atomic oxidation states. Based on the photoelectric effect discovered by H. R. Hertz in 1887 and explained by A. Einstein in 1905, it allows one to probe a range of electronic states in atoms comprising materials or molecules. The basic process is shown in the schematic below. A source provides a beam of X-rays of frequency v which impinges on the surface of a sample; electrons are subsequently excited from bound to empty states in the system and leave the sample under the influence of an external electric field. By measuring the kinetic energies K of such photoelectrons, the binding energies E_b of the initial states are determined via Einstein's formula: $E_\mathrm{b} = K - hv - \Phi$, where Φ is the work function of the sample. The frequency of the X-rays determines which electronic states are probed and how deep within the sample the photons can penetrate. It is therefore possible, by varying the frequency, to probe states varying from the valence band to deep within the atomic core. Moreover, lower frequencies allow one to analyse surface electronic states (so-called soft XPS), while high frequencies are used to probe states within the bulk of the sample (hard XPS).
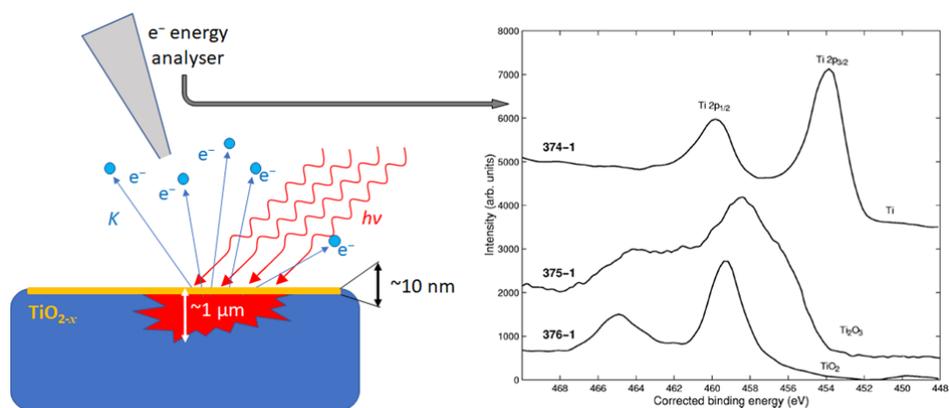
The theory of the process developed by K. Siegbahn considers the effect of both the initial and final state of the excited electron, and relates the quantised bands in the observed spectroscopic signatures to the "true" electron energies in the material, which are characteristic of particular elements in particular chemical states. By calibrating the experimental detectors against known 'reference' samples, one can determine chemical shifts in certain bands that arise due to changes in the chemical environment. For example, a change in the oxidation state of Ti between that in its metallic phase to the fully oxidised form of TiO_2 results in an observed shift of 4.6 eV in its 2p core levels, as shown in the schematic, where the data are taken from Ref. [56]. The XPS measurements employed to distinguish chemical elements and their electronic states are often referred to as Electron Spectroscopy for Chemical Analysis, or ESCA.

Care should be taken in the experimental setup regarding sample preparation, where charging effects will influence the observed work function and where surface inhomogeneity will give rise to specific spectroscopic signatures. As the chemical environment around atoms of interest will affect both the energy and line shapes, and a number of electronic terms may coexist even within one oxidation state, curve fitting procedures are applied to separate individual contributions. Such analysis yields valuable information about the chemical nature of the material's constituent elements. Moreover,

437 the electronic state of an atom/ion in the material may experience fluctuations, and will do
438 so necessarily in metals either intrinsically or upon a local photoexcitation during the
439 measurement. If the time of fluctuation is small, (for example in intra-ionic processes) only
440 the line shape will change. For long times (characteristic of inter-ionic charge transfer
441 processes), however, the XPS measurement can resolve different oxidation states and
442 involved electronic terms.
443

444   **References**

445   1.   Karen, P. Oxidation state, a long-standing issue! *Angew. Chemie - Int. Ed.* **54,** 4716–
446   4726 (2015).
447   2.   IUPAC gold book. Available at: https://goldbook.iupac.org/O04365.html.
448   3.   Goodman, C. H. L. Ionic-covalent bonding in crystals. *Nature* **187,** 590–591 (1960).
449   4.   Mooser, E. & Pearson, W. B. The ionic character of chemical bonds. *Nature* **1920,**
450   406–408 (1961).
451   5.   Cochran, W. 'Effective' ionic charge in crystals. *Nature* **191,** 60–61 (1961).
452   6.   Catlow, C. R. A. & Stoneham, A. M. Ionicity in solids. *J. Phys. C Solid State* **16,** 4321–
453   4338 (1983).
454   7.   Raebiger, H., Lany, S. & Zunger, A. Charge self-regulation upon changing the oxidation
455   state of transition metals in insulators. *Nature* **453,** 763–766 (2008).
456   8.   Jansen, M. & Wedig, U. A piece of the picture - misunderstanding of chemical
457   concepts. *Angew. Chemie - Int. Ed.* **47,** 10026–10029 (2008).
458   9.   Koch, D. & Manzhos, S. On the charge state of titanium in titanium dioxide. *J. Phys.*
459   *Chem. Lett.* **8,** 1593–1598 (2017).
460   10.   Walsh, A., Sokol, A. A., Buckeridge, J., Scanlon, D. O. & Catlow, R. A. Electron counting
461   in solids: oxidation states, partial charges, and ionicity. *J. Phys. Chem. Lett.* **8,** 2074–
462   2075 (2017).
463   11.   Pauling, L. The modern theory of valency. *J. Chem. Soc.* 1461–1467 (1948).
464   12.   Massidda, S., Yu, J., Freeman, A. J. & Koelling, D. D. Electronic structure and
465   properties of yba2cu3o7-δ, a low dimensional, low density of states superconductor.
466   *Phys. Lett. A* **122,** 198–202 (1987).
467   13.   Kageyama, H. *et al.* Expanding frontiers in materials chemistry and physics with
468   multiple anions. *Nat. Commun.* **9,** 772 (2018).
469   14.   Zhang, J. *et al.* Designing high-performance layered thermoelectric materials through
470   orbital engineering. *Nat. Commun.* **7,** 10892 (2016).
471   15.   Zeier, W. G. *et al.* Engineering half-heusler thermoelectric materials using zintl
472   chemistry. *Nat. Rev. Mater.* **1,** 16032 (2016).
473   16.   Gillespie, R. J. The valence-shell electron-pair repulsion (vsepr) theory of directed
474   valency. *J. Chem. Educ.* **40,** 295 (1963).
475   17.   Griffith, J. & Orgel, L. Ligand-field theory. *Q. Rev.* **11,** 381 (1957).
476   18.   Cockayne, E., Levin, I., Wu, H. & Llobet, A. Magnetic structure of bixbyite α-mn2o3: a
477   combined dft+u and neutron diffraction study. *Phys. Rev. B* **87,** 184413 (2013).
478   19.   Xiong-Fei Shen, † *et al.* A magnetic route to measure the average oxidation state of
479   mixed-valent manganese in manganese oxide octahedral molecular sieves (oms).
480   (2005). doi:10.1021/JA043406A
481   20.   Dirac, P. A. M. Quantum mechanics of many-electron systems. *Proc. R. Soc. London A*
482   *Math. Phys. Eng. Sci.* **123,** 714 (1929).
483   21.   Szabo, A. & Ostlund, N. S. *Modern quantum chemistry : introduction to advanced*
484   *electronic structure theory*. (Dover Publications, 1996).
485   22.   Mcweeny, R. The density matrix in many-electron quantum mechanics. i. generalized
486   product functions. factorization and physical interpretation of the density matrices.
487   *Proc. R. Soc. Lond. A. Math. Phys. Sci.* **253,** 242–259 (1959).
488   23.   Kantorovich, L. N. & Zapol, B. P. A diagram technique for nonorthogonal electron
489   group functions. i. right coset decomposition of symmetric group. *J. Chem. Phys.* **96,**
490   8420–8426 (1992).
491   24.   Bader, R. F. W. & Nguyen-Dang, T. T. Quantum theory of atoms in molecules-dalton

492   revisited. *Adv. Quantum Chem.* **14,** 63–124 (1981).

493 25. Kohn, W. Analytic properties of bloch waves and wannier functions. *Phys. Rev.* **115,**
494   809–821 (1959).

495 26. Marzari, N. & Vanderbilt, D. Maximally localized generalized wannier functions for
496   composite energy bands. *Phys. Rev. B* **56,** 12847–12865 (1997).

497 27. Mulliken, R. S. Electronic population analysis on lcao–mo molecular wave functions. i.
498   *J. Chem. Phys.* **23,** 1833–1840 (1955).

499 28. Christoffersen, R. E. & Baker, K. A. Electron population analysis. gross atomic charges
500   in molecules. *Chem. Phys. Lett.* **8,** 4–9 (1971).

501 29. Hirshfeld, F. L. Bonded-atom fragments for describing molecular charge densities.
502   *Theor. Chim. Acta* (1977). doi:10.1007/BF00549096

503 30. Becke, A. D. & Edgecombe, K. E. A simple measure of electron localization in atomic
504   and molecular systems. *J. Chem. Phys.* **92,** 5397–5403 (1990).

505 31. Savin, A. *et al.* Electron localization in solid-state structures of the elements: the
506   diamond structure. *Angew. Chemie Int. Ed. English* **31,** 187–188 (1992).

507 32. Dick, B. G. & Overhauser, A. W. Theory of the dielectric constants of alkali halide
508   crystals. *Phys. Rev.* **112,** 90 (1958).

509 33. Spaldin, N. A. A beginners guide to the modern theory of polarization. *J. Solid State*
510   *Chem.* **195,** 2–10 (2012).

511 34. King-Smith, R. D. & Vanderbilt, D. Theory of polarization of crystalline solids. *Phys.*
512   *Rev. B* (1993). doi:10.1103/PhysRevB.47.1651

513 35. Jiang, L., Levchenko, S. V. & Rappe, A. M. Rigorous definition of oxidation states of
514   ions in solids. *Phys. Rev. Lett.* **108,** 166403 (2012).

515 36. Day, P., Hush, N. S. & Clark, R. J. H. Mixed valence: origins and developments. *Philos.*
516   *Trans. A. Math. Phys. Eng. Sci.* **366,** 5–14 (2008).

517 37. Robin, M. B. & Day, P. Mixed valence chemistry-a survey and classification. *Adv.*
518   *Inorg. Chem. Radiochem.* **10,** 247–422 (1968).

519 38. Allen, J. P., Scanlon, D. O. & Watson, G. W. Electronic structure of mixed-valence
520   silver oxide ago from hybrid density-functional theory. *Phys. Rev. B* **81,** 161103
521   (2010).

522 39. Conejeros, S., Moreira, I. de P. R., Alemany, P. & Canadell, E. Nature of holes,
523   oxidation states, and hypervalency in covellite (cus). *Inorg. Chem.* **53,** 12402–12406
524   (2014).

525 40. Senn, M. S., Wright, J. P. & Attfield, J. P. Charge order and three-site distortions in the
526   verwey structure of magnetite. *Nature* **481,** 173–176 (2012).

527 41. Oganov, A. R. *et al.* Ionic high-pressure form of elemental boron. *Nature* **457,** 863–
528   867 (2009).

529 42. Albers, R. C. Condensed-matter physics: an expanding view of plutonium. *Nature* **410,**
530   759–761 (2001).

531 43. Janoschek, M. *et al.* The valence-fluctuating ground state of plutonium. *Sci. Adv.* **1,**
532   e1500188 (2015).

533 44. Watanabe, S. & Miyake, K. Quantum valence criticality as an origin of unconventional
534   critical phenomena. *Phys. Rev. Lett.* **105,** 186403 (2010).

535 45. Watanabe, S. & Miyake, K. Roles of critical valence fluctuations in ce- and yb-based
536   heavy fermion metals. *J. Phys. Condens. Matter* **23,** 094217 (2011).

537 46. Yamaoka, H. *et al.* Role of valence fluctuations in the superconductivity of ce122
538   compounds. *Phys. Rev. Lett.* **113,** 086403 (2014).

539 47. Putzke, C. *et al.* Anomalous critical fields in quantum critical superconductors. *Nat.*

540   *Commun.* **5,** 5679 (2014).

541   48.   Mondal, S. *et al.* Experimental evidence of orbital order in α -b 12 and γ -b 28

542   polymorphs of elemental boron. *Phys. Rev. B* **88,** 024118 (2013).

543   49.   Nilsson Pingel, T., Jørgensen, M., Yankovich, A. B., Grönbeck, H. & Olsson, E. Influence

544   of atomic site-specific strain on catalytic activity of supported nanoparticles. *Nat.*

545   *Commun.* **9,** 2722 (2018).

546   50.   Anasori, B., Lukatskaya, M. R. & Gogotsi, Y. 2D metal carbides and nitrides (mxenes)

547   for energy storage. *Nat. Rev. Mater.* **2,** 16098 (2017).

548   51.   Jiang, B., Zuo, J. M., Jiang, N., O'Keeffe, M. & Spence, J. C. H. Charge density and

549   chemical bonding in rutile, tio2. *Acta Crystallogr. Sect. A Found. Crystallogr.* **59,** 341–

550   350 (2003).

551   52.   Scanlon, D. O. *et al.* Band alignment of rutile and anatase tio2. *Nat. Mater.* **12,** 798–

552   801 (2013).

553   53.   Burdett, J. K. Structural–electronic relationships in rutile. *Acta Crystallogr. Sect. B* **51,**

554   547–558 (1995).

555   54.   Morgan, B. J. & Watson, G. W. A density functional theory + *u* study of oxygen

556   vacancy formation at the (110), (100), (101), and (001) surfaces of rutile tio $_2$. *J. Phys.*

557   *Chem. C* **113,** 7322–7328 (2009).

558   55.   Brown, I. D. (Ian D. *The chemical bond in inorganic chemistry : the bond valence*

559   *model*. (Oxford University Press, 2002).

560   56.   Kurtz, R. L. & Henrich, V. E. Comparison of ti 2p core-level peaks from tio2, ti2o3, and

561   ti metal, by xps. *Surf. Sci. Spectra* **5,** 179 (1998).

562

563 **Correspondence and requests for materials should be addressed to** A. W.

564   (a.walsh@imperial.ac.uk) or C. R. A. C. (c.r.a.catlow@ucl.ac.uk).

565

570

571 **Author contributions** All authors contributed equally to the design, writing and editing of

572 the manuscript.

573

574 **Competing interests** The authors declare no competing interests.

a Free Atoms

O $1s^2 2s^2 2p^4$

Ti $[Ar]3d^2 4s^2$

Free Ions

O^{2-} $\xrightarrow{4e^-}$ Ti^{4+}

$1s^2 2s^2 2p^6$ $[Ar]3d^0 4s^0$

b Rutile TiO_2

$r_1 > r_2$ (D_{4h} symmetry)
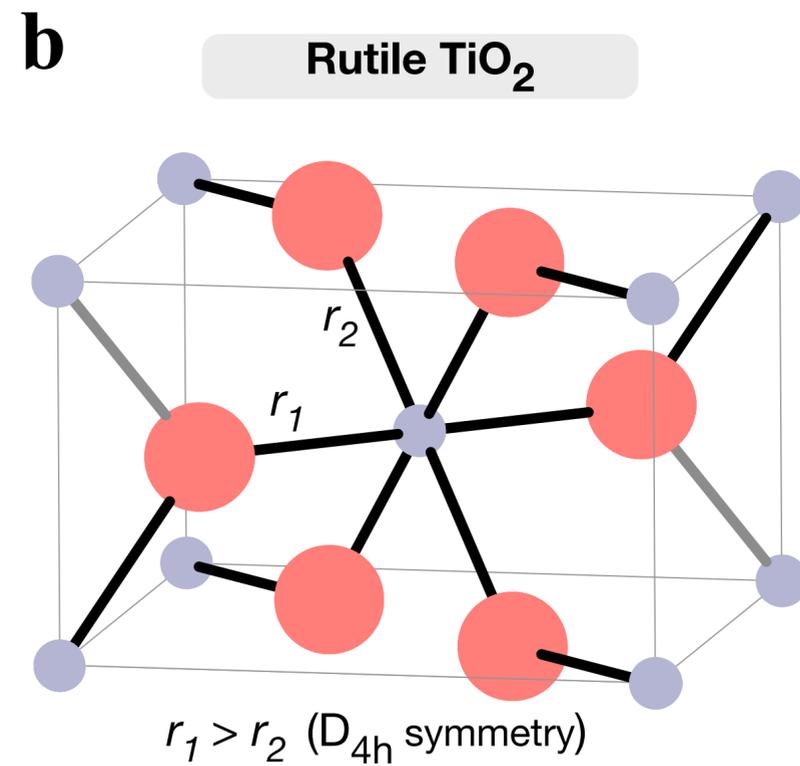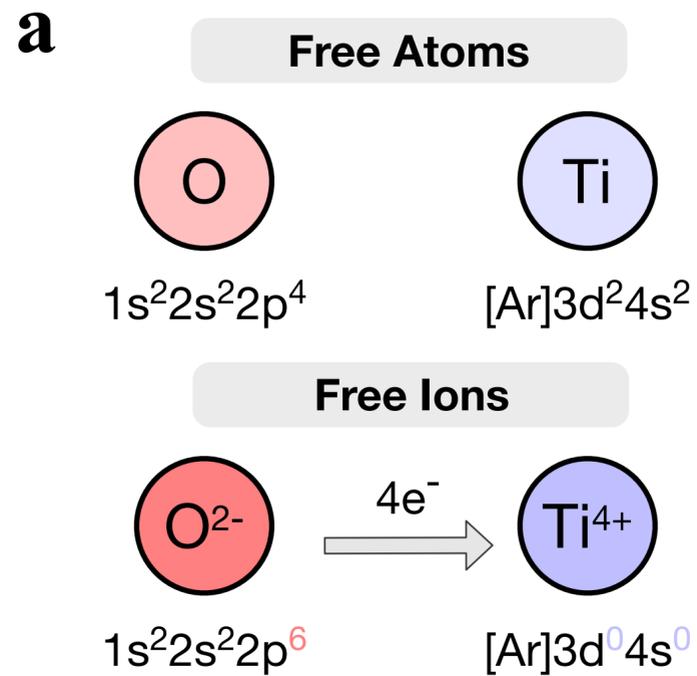
**c** Probes of Charge Distribution

|	
Structural	Consistent with d^0 Ti: no Jahn-Teller distortion
Vibrational	Large $\omega_{LO} / \omega_{TO}$ splitting: E_u = 494 / 842 cm^{-1}
Electronic	X-ray photoemission: O 2p upper valence band
Dielectric	Born effective charge tensor of Ti: +5 to +7
Magnetic	Diamagnetic Ti(IV); paramagnetic Ti(III) on reduction
Optical	Transparent crystal: 3.2 eV excitation from O to Ti
Chemical	No further oxidation from TiO_2

d Charge Density Difference
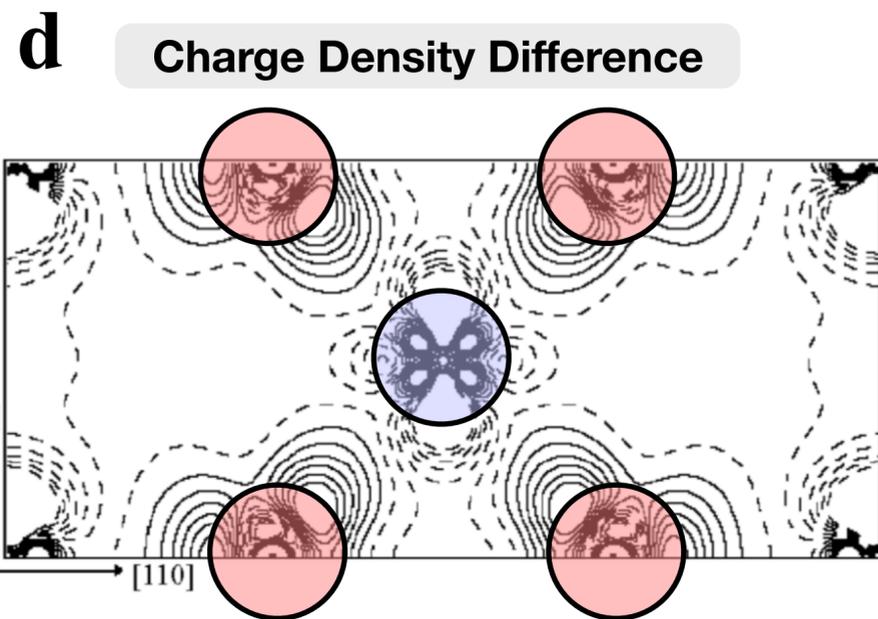
Combined from X-ray and electron diffraction with respect to neutral atoms

e Electronic Density of States

Valence band

Conduction band

Total DOS

Ti s

O p

Ti p

Ti d

Energy (eV)
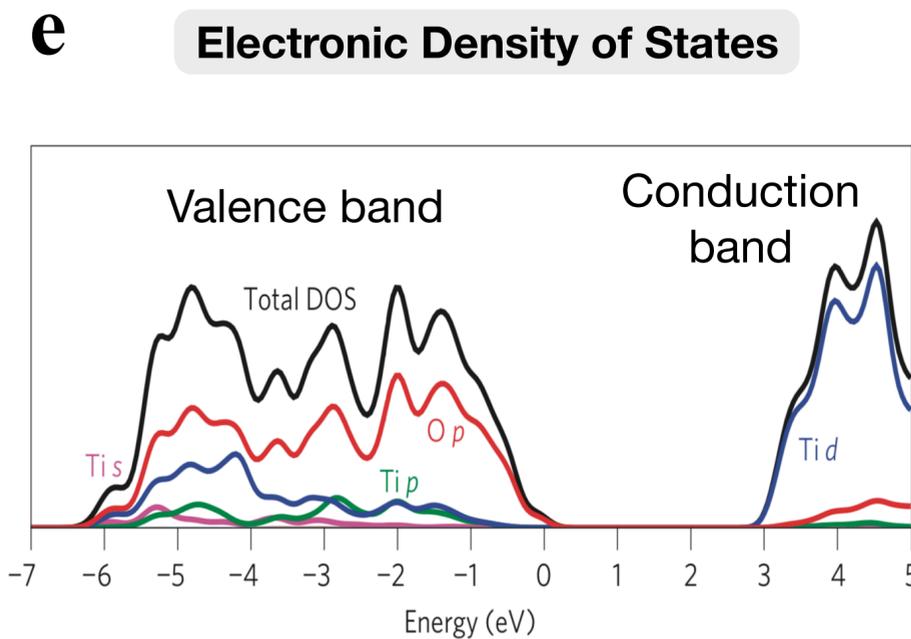
Density functional theory calculations confirms Ti 3d conduction band

f

Ti-O σ^* 8e

Ti-O σ^* 16e

Ti-O π^* 4e

Ti-Ti π^* 2e

Ti-Ti π 2e

Ti-Ti σ^* 2e

Ti-Ti σ 2e

O-p_z π 4e

Ti-O π 4e

Ti-O σ 16e

Ti-O σ 8e

$e_g^2 sp^3$

d_{xz}

$d_{x^2-y^2}$

d_{yz}

p_z

p_x, p_y

s
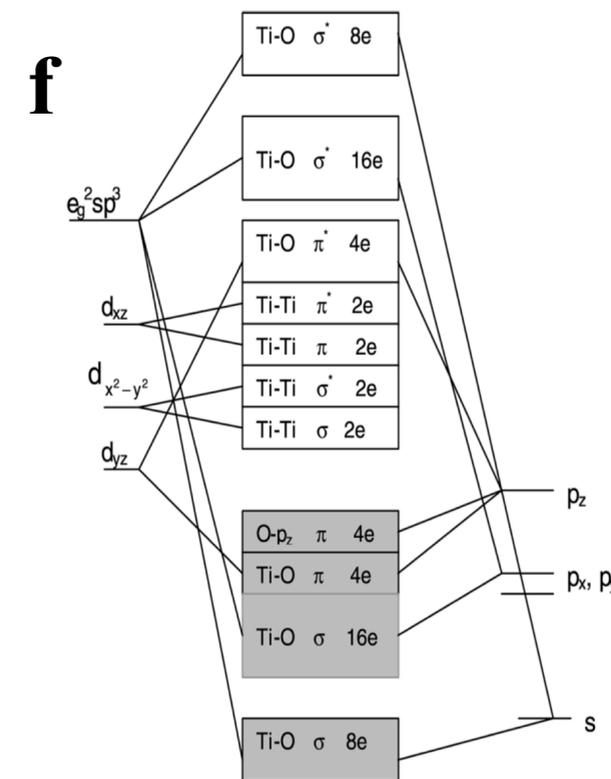
Molecular orbital scheme describing hybridisation between O (left) and Ti (right)

Reduced Ti(III) on Surface

(100)

60°
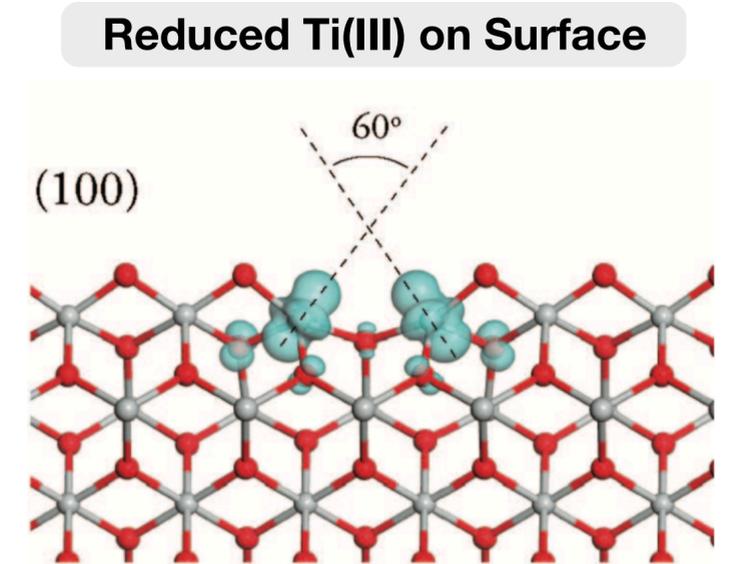
Oxygen vacancy generates two Ti(III) d^1 centres

Geometric Partitioning
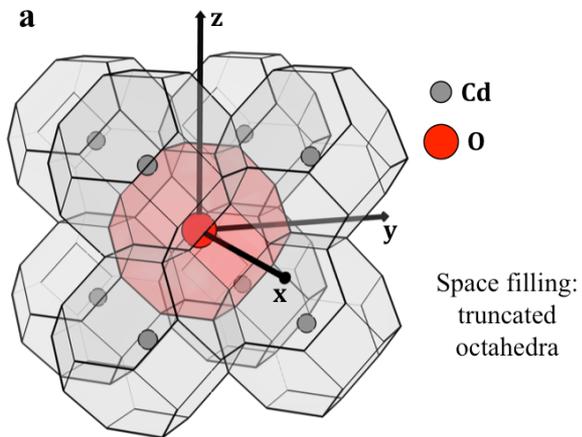
a

Cd
O

Space filling:
truncated
octahedra

Bader Partitioning

b

Cd

O

$\nabla\rho(\vec{r})=0$

Electron Localisation Function (ELF)

c

Cd

O

0.8

0.4

0

$$\text{ELF}=\left\{1+\left[\frac{C(\vec{r})}{C_h(\rho(\vec{r}))}\right]^2\right\}^{-1}$$

Modern Theory of Polarisation

d

$\Delta\mathbf{p}_{\text{ion}}$

$\Delta\mathbf{p}_{\text{elec}}$

$$\Delta\mathbf{p}_{\text{elec}}\propto\sum_n\left\{\int_{\text{BZ}}d\mathbf{k}\,\mathrm{e}^{-i\mathbf{k}\cdot\mathbf{R}}\left[\left\langle u_{n\mathbf{k}}^f\left|\frac{\partial u_{n\mathbf{k}}^f}{\partial\mathbf{k}}\right.\right\rangle-\left\langle u_{n\mathbf{k}}^0\left|\frac{\partial u_{n\mathbf{k}}^0}{\partial\mathbf{k}}\right.\right\rangle\right]\right\}$$

"Berry phase"
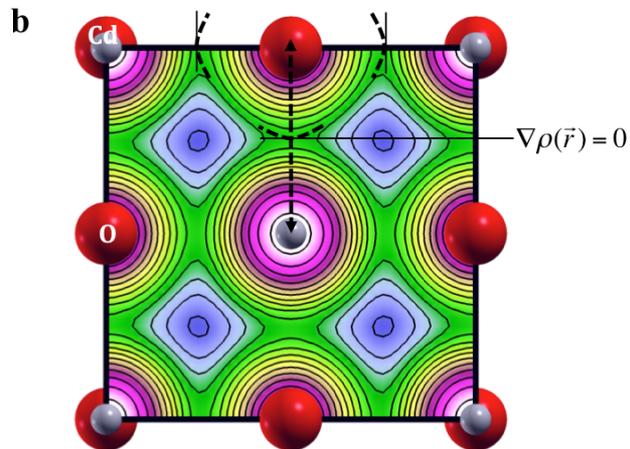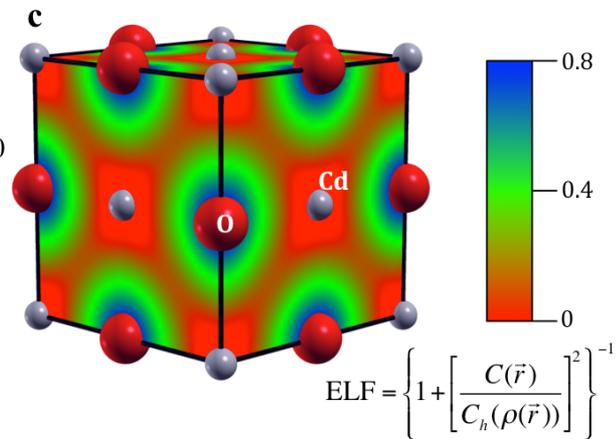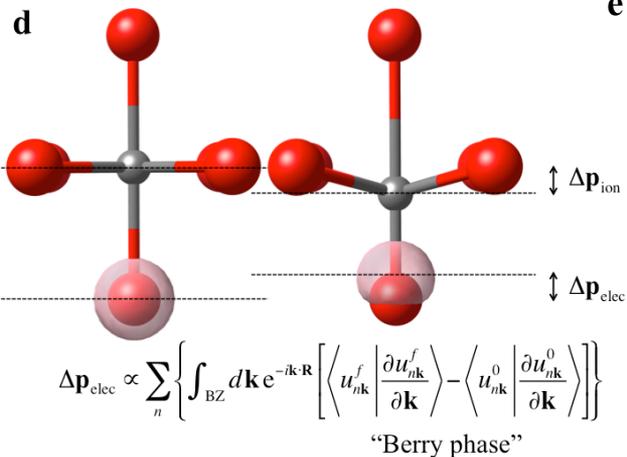
Atomic Orbital-Based Partitioning

e

Wannier function
representation: projected to
atomic orbitals

$$w(r)\sim\int_{\text{BZ}}d\mathbf{k}\,\mathrm{e}^{-i\mathbf{k}\cdot\mathbf{R}}\,\psi_{n\mathbf{k}}(r)$$

s p_x p_y p_z

d_{xy} d_{xz} d_{yz} $d_{x^2-y^2}$ d_{z^2}

Combined: charge density in
extended system

'Overlap'